

Pacific Decadal Variability in the View of Linear Equatorial Wave Theory*

JULIEN EMILE-GEAY AND MARK A. CANE

Lamont-Doherty Earth Observatory, Columbia University, Palisades, New York

(Manuscript received 6 March 2007, in final form 3 June 2008)

ABSTRACT

It has recently been proposed, within the framework of the linear shallow-water equations, that tropical Pacific decadal variability (PDV) can be accounted for by basin modes with eigenperiods of 10 to 20 yr, amplifying a midlatitude wind forcing with an essentially white spectrum. Here the authors use a different formalism of linear equatorial wave theory. The Green's function is computed for the wind-forced response of a linear equatorial shallow-water ocean and uses the earlier results of Cane and Moore to obtain a compact, closed form expression for the motion of the equatorial thermocline, which applies to all frequencies lower than seasonal. This expression is new and allows a systematic comparison of the effect of low- and high-latitude winds on the equatorial thermocline. At very low frequencies (decadal time scales), the planetary geostrophic solution used by Cessi and Louazel is recovered, as well as the equatorial wave solution of Liu, and a formal explanation for this convergence is given. Nonetheless, this more general solution leads one to a different interpretation of the results. In contrast to the aforementioned studies, the authors find that the equatorial thermocline is inherently more sensitive to local than to remote wind forcing and that planetary Rossby modes only weakly alter the spectral characteristics of the response. Tropical winds are able to generate a strong equatorial response with periods of 10 to 20 yr, while midlatitude winds can only do so for periods longer than about 50 yr. The results suggest that ocean basin modes are an unlikely explanation of decadal fluctuations in tropical Pacific sea surface temperature.

1. Introduction

The existence of decadal-scale variability in the Pacific Ocean is now well documented, and it affects the climate and fisheries of the neighboring regions to a significant extent (e.g., Trenberth and Hurrell 1994; Zhang et al. 1997; Mantua et al. 1997). This Pacific decadal variability (PDV) in the North Pacific is usually described by the Pacific decadal oscillation (PDO) index (Mantua and Hare 2002), which is quite energetic in the interdecadal spectral range.

There have been suggestions (e.g., Newman et al. 2003) that the PDV derives much of its characteristics from the decadal properties of the El Niño–Southern Oscillation (ENSO), notwithstanding feedbacks with

subtropical and midlatitudes winds, which may have a significant role in amplifying decadal variability over the whole basin (Sarachik and Vimont 2003). Hence, rather than asking “Why is there a PDV?,” it is worthwhile to ask the more fundamental question of why there are decadal SST variations in the tropical Pacific.

To describe such variations, one can look at the so-called cold tongue index (CTI) (Deser and Wallace 1990), computed here from the historical SST analysis of Kaplan et al. (1998). The index and its spectrum are shown in Fig. 1. The spectrum was estimated via the multitaper method (Thomson 1982; Ghil et al. 2002) and the robust noise estimation procedure of Mann and Lees (1996). At the 95% level, one can see a number of significant broadband peaks between periods 2 and 7 yr, as well as narrowband peaks in the quasi-biennial and quasi-quadrennial range (Jiang et al. 1995), all of which compose ENSO. One also finds some peaks in the decadal-to-multidecadal range, none of which seems to rise above the red noise background used for significance testing, perhaps due to the shortness of the record.

Thus, for our purpose, the salient feature tropical Pacific SST variability is the overall warm color of its

* Lamont-Doherty Earth Observatory Contribution Number 7210.

Corresponding author address: Julien Emile-Geay, School of Earth and Atmospheric Sciences, Georgia Institute of Technology, Ford ES&T Room 2248, 311 Ferst Drive, Atlanta, GA 30332-0340.
E-mail: julien@gatech.edu

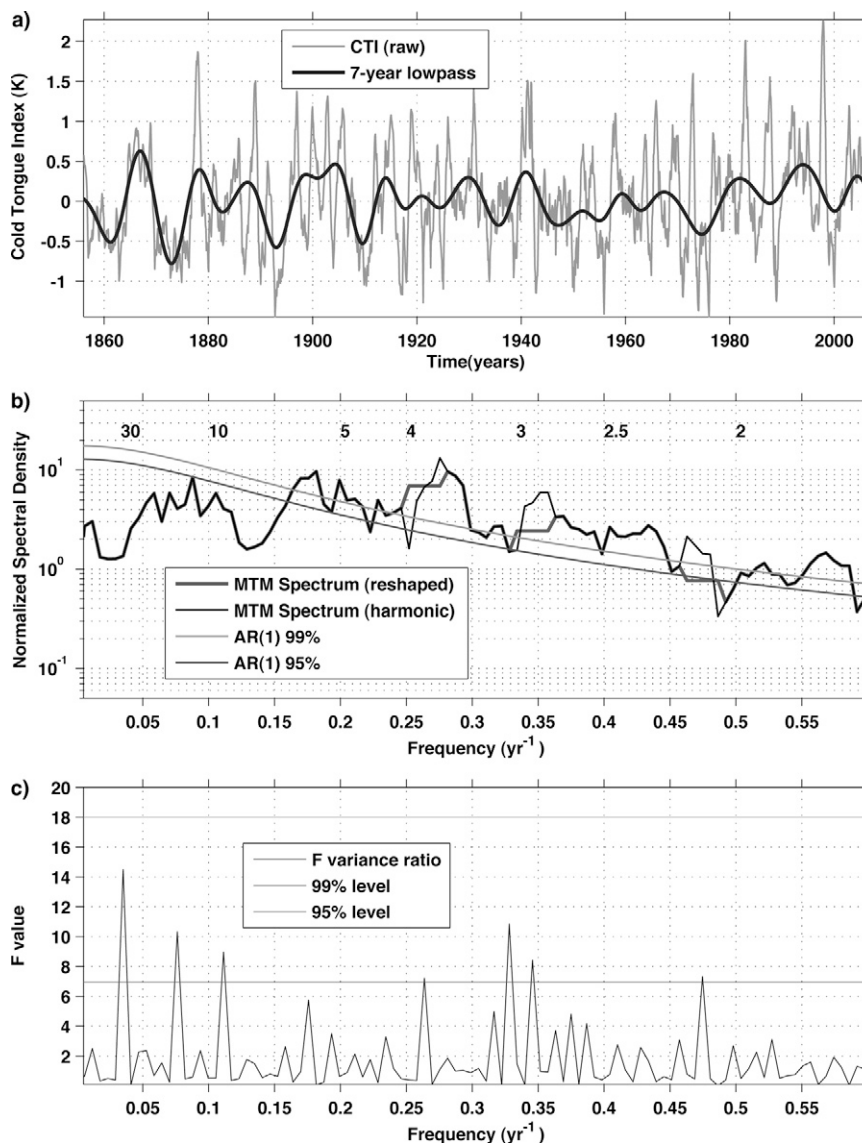


FIG. 1. The cold tongue index (CTI) and its spectral properties: (a) CTI and its 7-yr low-pass-filtered version; (b) spectral estimate of the CTI using multitaper method (MTM) and the robust noise estimation procedure of Mann and Lees (1996). The black curve identifies harmonic components together with noise and broadband signals, while the “reshaped” spectrum only includes the latter two. Numbers above the curves correspond to the period (yr) of oscillation. (c) Significance test of harmonic components, based upon an F test (Mann and Lees 1996). A peak is deemed significant if its F value is above the critical threshold imposed by a particular confidence level (95% or 99% here).

spectrum at low frequencies. An intriguing mechanism for this variability has recently been proposed in the work of Cessi and collaborators (Cessi and Louazel (2001, hereafter CL01), Cessi and Primeau (2001), Cessi and Paparella (2001), and that of Liu (2003, hereafter L03) in the framework of the linear shallow-water equations.

These authors made an attempt to explain decadal variability as a “reddening” of weather fluctuations by

dynamical ocean processes—planetary basin modes in this case. They argue that, in a meridionally bounded basin, such modes with decadal time scales can be preferentially excited by the appropriate wind forcing in midlatitudes, resulting in a large local response and a somewhat weaker—but still sizable—equatorial response. The wind need not be highly organized; the usual “white noise” variations in midlatitudes might be all that is needed. Moreover, this scenario does open

the possibility of tropical anomalies forcing teleconnections to higher latitudes that excite favorable winds, reinforcing the decadal mode of variation (Cessi and Paparella 2001). Cessi and collaborators work with the linear planetary geostrophic equations, while L03, following Jin (2001), uses a truncated series of equatorial waves. L03 shows that the two approaches yield the same results. However, the latter are highly dependent on a few functional forms chosen to exemplify the forcing, which prevents rigorous comparison between the influence of low- and high-latitude forcing.

We therefore approach the problem in a different way, one that relies heavily on results obtained by Cane and Moore (1981, hereafter CM81) and Cane and Sarachik (1981, hereafter CS81) to derive the Green's function of the problem in a closed basin. We obtain answers that are mathematically equivalent to those of CL01 and L03, but our approach leads us to an interpretation at odds with theirs. Most importantly, we find that high-latitude winds have no advantage in forcing tropical ocean motions. On the contrary, they are typically less effective than low-latitude winds.

Since it is all too easy for the reader to get lost in the mathematical details, it may be worthwhile to give a brief informal account of the approach we will take. We wish to find the ocean's response to a periodic wind forcing. As in CS81, we write the solution as a sum of a forced part and a free part. Both are made up of forced or free long equatorial Kelvin waves and long Rossby waves, the only modes that exist in the interior of the basin at low frequencies. These modes suffice to satisfy the boundary condition of vanishing zonal velocity at the east, but cannot satisfy the same boundary condition at the west. That requires the short Rossby waves that make up the western boundary currents. It is known (Cane and Sarachik 1977) that the appropriate boundary condition for the long, low frequency waves alone is that the meridional integral of the zonal velocity vanish along the boundary. This means that the mass propagated into the western boundary by long Rossby waves forced by the wind is all returned to the interior in free equatorial Kelvin waves; this condition determines the Kelvin wave amplitude at the west. The role of the short Rossby waves (the western boundary currents) is to close the fluid circuits.

The free Kelvin waves, generated at the western boundary, and the Kelvin wave forced in the interior propagate eastward to be reflected in a series of Rossby waves, whose amplitudes are determined by the boundary condition at the east. These Rossby waves propagate across to the west and generate new Kelvin waves, and so on. A Kelvin wave plus its reflected Rossby waves is the free part of our solution. There is some

amplitude A for this free part that allows the forced plus free Rossby wave mass flux incident on the western boundary to just balance the outgoing Kelvin wave mass flux.

It turns out (section 2a) that A is the correct measure of off-equatorial wind effects on the equatorial thermocline, being equal to the thermocline depth at the eastern boundary (h_E). Clearly, the greater the amplitude of the wind-forced mass flux at the western boundary, the greater h_E will be. So, the right forcing can increase the movement of the equatorial thermocline. There is a second mechanism, which depends on the free mode. If the free mode were self-consistent so that the Kelvin wave generated at the west reflects into Rossby waves that are exactly what is needed to generate that Kelvin wave in the first place, then it would be a self-sustained basin mode, a complete solution of the unforced equations in the basin: a resonant mode. If the free mode is close to this condition, then it adds little net mass flux at the west and it will take a large amplitude of h_E to complete the forced solution.

Hence the emphasis on basin modes in the work cited above. However, even in the absence of any friction, it is known that there are no true very-low-frequency basin modes; there are no eigenfunctions satisfying the shallow-water equations and the boundary conditions whose eigenfrequencies are real (Moore 1968). The only solutions have complex eigenfrequencies, meaning that the associated quasi-basin modes are damped (Cessi and Louazel 2001).

Thus, to determine what sort of midlatitude winds might excite a large equatorial response means that we have to investigate two questions: What latitudinal distribution of winds is especially efficient at forcing a large net mass flux at the western boundary? What frequencies and basin dimensions bring the free mode close to resonance? It should be noted that since any free mode must satisfy the eastern boundary condition, the free mode we describe here—a Kelvin wave at frequency ω together with its eastern boundary reflected Rossby waves—is the only possible form for a low-frequency basin mode. Its form is the same as that found numerically by CL01 and L03. Here we add a closed form description, which takes advantage of the analytical results of CM81.

In the next section, we present the mathematical formalism used to address this problem. In particular, we modify the CM81 mode to fit in a meridionally bounded basin and calculate h_E when the forcing is a delta function in latitude (a Green's function). This allows a systematic investigation of the effect of forcing latitude, which we do in section 3. Those results are compared with previous work in section 4 and we offer

an explanation for the differences we find. We conclude with a discussion section.

2. Linear equatorial wave theory at decadal frequencies

a. The problem

Consider an ocean basin defined by $\{0 \leq x \leq X_E; y_S \leq y \leq y_N\}$. We start from the classical reduced-gravity model, with the nondissipative rotating shallow-water equations, in the low-frequency, long-wave approximation (e.g., Moore 1968; Cane and Sarachik 1976). In nondimensional form

$$u_t - yv + h_x = \tau_x, \quad (1a)$$

$$yu + h_y = \tau_y, \quad (1b)$$

$$h_t + u_x + v_y = 0 \quad (1c)$$

with boundary conditions (Cane and Sarachik 1977)

$$u(X_E, y, t) = 0 \quad \forall y \in [y_S; y_N], \quad (2a)$$

$$\int_{y_S}^{y_N} u(x=0) dy = 0. \quad (2b)$$

As a consequence of the low-frequency, long-wave approximation, the v_t term is absent and the boundary condition (2b) has to include the indirect effect of the short Rossby waves, as discussed above. As in CS81, we consider periodic wind perturbations (tantamount to solving in the frequency domain) and further idealize them as strictly zonal and independent of longitude: $\boldsymbol{\tau} = [F(y)e^{i\omega t}, 0]$. This functional form facilitates comparison with CS81, L03, and CL01.

The solution to this system is a sum of forced Rossby and Kelvin waves, together with their reflections, which are free waves. As is often done (e.g., CS81) the solution is written as the sum of a forced solution \mathbf{u}_F of (1) and a free solution \mathbf{u}_M [i.e., one satisfying (1) with the right-hand side set to zero]:

$$\mathbf{u} = (u, v, h)^T = \mathbf{u}_F + A\mathbf{u}_M, \quad (3)$$

where $A(t)$ is a function of time only, determined by the boundary conditions.

Both the forced and free parts satisfy the boundary condition (2a) at the east. We normalize $\mathbf{u}_M = (u_M, v_M, h_M)^T$ so that $h_M(x = X_E, y) = 1$. In the absence of meridional wind stress, the meridional momentum balance reduces to geostrophy and the boundary condition $u(X_E, y) = 0$ implies that $h(X_E, y) = h_E(t)$, a function of time only.

It turns out that $A = h_E$, which is entirely determined by the condition (2b) that the net mass flux be zero at the west. After substituting (3) into (2b), a few manipulations lead to

$$h_E = -\frac{I_F}{I_M}, \quad (4)$$

where $I_M \equiv \int_{y_S}^{y_N} u_M(x=0) dy$ and $I_F \equiv \int_{y_S}^{y_N} u_F(x=0) dy$.

The depth h_E is also the physical variable of greatest interest because the eastern equatorial SST is so tightly coupled to the local thermocline depth (e.g., Zelle et al. 2004, and references therein). As noted above, if the wind forcing is far from the equator, then all variations in h along the equator are determined solely by h_E . The rest of the analysis will thus focus on this variable.

As is apparent from (4), any mode rendering I_M small will generate a large response in thermocline depth, regardless of the magnitude of the forcing. If $I_M = 0$, then \mathbf{u}_M is a true basin mode, as in CM81, and we therefore begin by seeking the free solutions to the system ($F = 0$).

b. The free mode

The general form for this mode is the sum of a Kelvin wave and all its Rossby reflections. To take advantage of prior work, we split the solution between a part corresponding to a meridionally infinite basin \mathbf{u}_M^∞ and a boundary layer correction \mathbf{u}_B . The first term \mathbf{u}_M^∞ can readily be written in the closed form obtained by CM81:

$$\begin{aligned} \mathbf{u}_M^\infty &= \begin{pmatrix} u_M^\infty \\ v_M^\infty \\ h_M^\infty \end{pmatrix}, \\ &= e^{i\omega t} \begin{pmatrix} -i \tan(2\phi\xi) \\ i\omega y \sec^2(2\phi\xi) \\ 1 \end{pmatrix} [\cos(2\phi\xi)]^{1/2} \exp\left(iy^2 \frac{\tan 2\phi\xi}{2}\right), \end{aligned} \quad (5)$$

wherein

$$\xi = \frac{x - X_E}{X_E}, \quad \phi = \frac{\omega X_E}{c}. \quad (6)$$

Here ξ goes from -1 in the west to 0 in the east and ϕ , which is 2π times the ratio of the Kelvin wave crossing time to the period of the oscillation, is the relevant frequency parameter for analysis of the response (CS81). For a meridionally infinite basin,

$$\begin{aligned} I_M &= \int_{-\infty}^{\infty} u_M^\infty(x=0) dy, \\ &= i \tan(2\phi) [\cos(2\phi)]^{1/2} \int_{-\infty}^{\infty} e^{-iy^2 (\tan 2\phi)/2} dy, \\ &= \sqrt{2\pi i \sin 2\phi}. \end{aligned} \quad (7)$$

For very low frequencies $\phi \ll 1$, $I_M \approx 2\sqrt{i\pi\phi}$.

A true basin mode must satisfy the boundary condition at the east; hence, in an infinite basin all low-frequency basin modes have the form (5). A basin mode must also satisfy the western boundary condition, $I_M = 0$. This will hold if ϕ is a multiple of $\pi/2$, a result first obtained by CM81. The longest eigenperiod is $4X_E$, the time for a Kelvin wave to cross the basin plus the time for the gravest Rossby wave to return (about 8 months for typical parameters). Thus, all true basin modes are high frequency compared to decadal (or even interannual) time scales. Any low frequency modes must correspond to complex eigenfrequencies and, so, will be damped.

The form of the phase function in (5) means that phase variations increase with latitude and with proximity to the western boundary. Hence, the most rapid variations are found in the northwestern and southwestern corners of the basin. If the modes are damped, then these areas will also have larger amplitudes. These characteristics may be seen in the basin modes shown by CL01 and L03 [their Fig. 2 and Fig. 2b, respectively].

In a bounded basin, (5) is still a free solution satisfying the boundary condition at the eastern boundary, but it fails to satisfy the boundary conditions at (y_S, y_N) . The complete solution requires the addition of boundary layers to make the meridional velocity vanish at those latitudes. All we need is the mass flux that they deliver to the western boundary, and this does not require complete knowledge of the structure within the boundary layer. (The boundary layer structure is discussed, for example, by CL01.)

Consider the situation at, say, the northern boundary $y = y_N$. We add a boundary layer structure \mathbf{u}^B to \mathbf{u}_M^∞ to satisfy the boundary condition at $y = y_N$ that $0 = v_M = v_M^\infty + v^B$. At low frequencies the narrow meridional scale of the boundary layer reduces the continuity equation to $u_x^B + v_y^B \approx 0$. Integrating this continuity equation from the east where $u^B = 0$ and noting that the boundary layer variables vanish far from the boundary,

$$\int_{-\infty}^{y_N} u_B(x=0) dy = \int_0^{X_E} [v_B]_{-\infty}^{y_N} dx, \tag{8}$$

$$= - \int_0^{X_E} v_M^\infty(y=y_N) dx,$$

which, using (5), is

$$\int_{-\infty}^{y_N} u_B(x=0) dy = -iy_N \int_{-\phi}^0 \sec^2(2s) e^{iy^2(\tan 2s)/2} ds \tag{9}$$

$$= \frac{-1}{y_N} [1 - e^{-iy_N^2(\tan 2s)/2}].$$

Similarly, at the southern boundary

$$\int_{y_S}^{\infty} u_B(x=0) dy = \frac{1}{y_S} [1 - e^{-iy_S^2(\tan 2\phi)/2}]. \tag{10}$$

We also have [cf. (7)]

$$\int_{y_S}^{y_N} u_M^\infty(x=0) dy, \tag{11}$$

$$= i \tan(2\phi) [\cos(2\phi)]^{1/2} \int_{y_S}^{y_N} e^{-iy^2(\tan 2\phi)/2} dy;$$

defining $\sigma = (\tan 2\phi)/2 \approx \phi$ and $\theta = \sigma y^2$, we may write

$$\int_{y_S}^{y_N} u_M^\infty(x=0) dy = 2(i\sigma)^{1/2} [\cos(2\phi)]^{1/2} \int_{\sqrt{i\theta_S}}^{\sqrt{i\theta_N}} e^{-s^2} ds \tag{12}$$

$$\approx 2(i\sigma)^{1/2} \int_{\sqrt{i\theta_S}}^{\sqrt{i\theta_N}} e^{-s^2} ds.$$

Here the subscripts N and S refer to the northern or southern boundary, respectively. Henceforth, we will use the last expression since the relative error is $\phi^2 + O(\phi^4)$, which is $\leq 1\%$ for the very low frequency motions ($\phi \ll 1$) of interest here. [For a 20-yr period and a basin the size of the Pacific, ($\phi \approx 0.06$).]

Now, rewriting (12) with the help of the error function

$$\text{erf}(x) = \frac{2}{\sqrt{\pi}} \int_0^x e^{-s^2} ds$$

(e.g., Abramowitz and Stegun 1965) and combining this with Eqs. (9) and (10), the total mass flux can be written:

$$I_M(\phi, y_N, y_S) = \sqrt{i\sigma} [Z(\sigma y_N^2) - \text{sgn}(y_S) Z(\sigma y_S^2)], \tag{13}$$

where we have introduced the function Z ,

$$Z(\theta) = \sqrt{\pi} \text{erf}(\sqrt{i\theta}) - \frac{1 - e^{-i\theta}}{\sqrt{i\theta}}. \tag{14}$$

If $I_M = 0$, then the free mode is a basin mode. This holds if $\sigma = 0$, but the only very-low-frequency solution is the steady solution $\phi = 0$. Otherwise, let $y_S = 0$ so that $I_M = 0$ reduces to $Z(\sigma y_N^2) = 0$, which is the same as Eq. (2.9) in L03. This is easily shown by integrating (14) by parts:

$$Z(\theta) = - \int_0^{\sqrt{i\theta}} \frac{1}{s} d(e^{-s^2}) - \frac{1 - e^{-i\theta}}{\sqrt{i\theta}}, \tag{15}$$

$$= \int_0^{\sqrt{i\theta}} \frac{1 - e^{-s^2}}{s^2} ds.$$

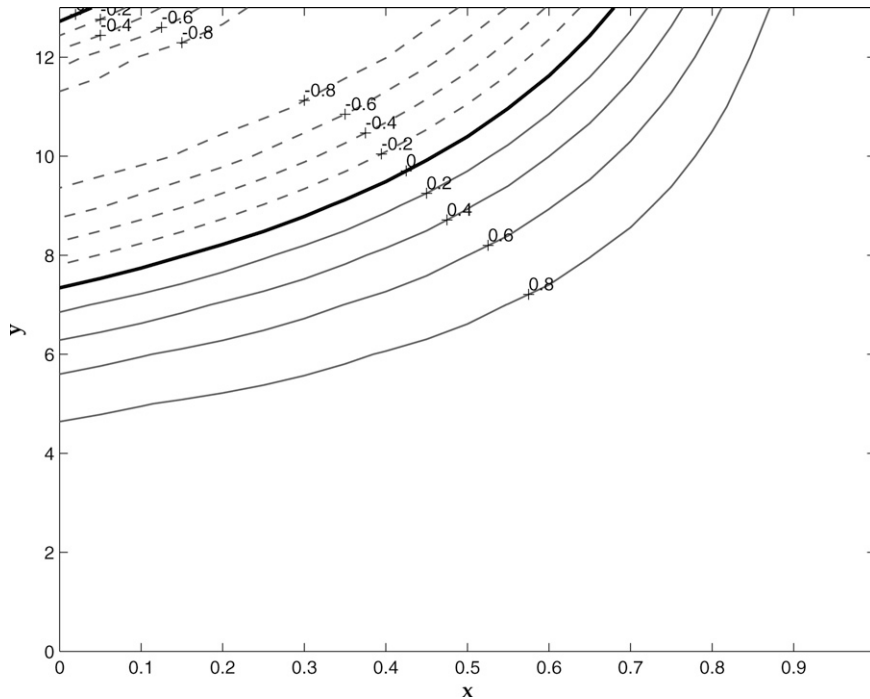


FIG. 2. Eigenstructure of the free mode h_M for $\beta\omega = -0.029$ to facilitate comparison with the gravest planetary basin mode of Yang and Liu (2003).

The solutions may be found numerically, as in CL01 and L03. The resulting eigenstructure, displayed in Fig. 2, is almost identical to that found by CL01 (their Fig. 2) and Yang and Liu (2003) (their Fig. 3).

The peculiar physics of equatorial wave propagation on a β plane further means that these modes can be described by a single parameter $\theta = \phi y^2$. It is worth dwelling on its physical interpretation as it appears repeatedly throughout this article. Recalling that the nondimensional Rossby phase speed at latitude y is $c(y) = y^{-2}$, θ can be interpreted as the ratio of the basin crossing time at latitude y to the period of interest (up to a factor of 2π); thus, for small θ the wave has had the time to go around the Kelvin–Rossby wave pathway before the signal has changed too much, and all latitudes equatorward of y are in phase; for large θ there are important phase differences, leading to interference.

We can obtain relatively simple asymptotic expressions for Z in these two interesting limits.

• For $\theta \ll 1$:

$$Z \sim Z_0 \equiv \sqrt{i\theta} \left(1 - \frac{i}{6}\theta - \frac{1}{30}\theta^2 \right), \quad (16)$$

which has amplitude

$$|Z_0| \sim \sqrt{\frac{\theta}{2}} \left(1 - \frac{7}{360}\theta^2 \right) \quad (17)$$

and phase

$$\varphi(Z_0) \sim \frac{\pi}{4} - \frac{\theta}{6}. \quad (18)$$

For $\theta \gg 1$:

$$Z \sim Z_\infty \equiv \sqrt{\pi} - \frac{1}{\sqrt{2\theta}} \left(1 + \frac{\sin\theta - \cos\theta}{2\theta} \right) - \frac{i}{\sqrt{2\theta}} \left(1 + \frac{\sin\theta + \cos\theta}{2\theta} \right), \quad (19)$$

which has amplitude

$$|Z_\infty| \sim \sqrt{\pi} - \frac{1}{\sqrt{2\theta}} + \frac{1}{4\sqrt{\pi\theta}} \quad (20)$$

and phase

$$\varphi(Z_\infty) \sim -\frac{1}{\sqrt{2\pi\theta}} - \frac{1}{3(2\pi\theta)^{3/2}}. \quad (21)$$

Taking (19) to the limit $\theta \rightarrow \infty$ by having $y_N = -y_S$ we find that, for $\theta \ll 1$, $I_M \sim 2(i\phi\pi)^{1/2}$, in agreement with

¹ Use the following asymptotic expansion: $\text{erf}(s) \sim 1 + (e^{-s^2}/\sqrt{\pi}) \sum_n (-1)^n [(2n-1)!!/2^n s^{2n+1}]$ with $(2n-1)!! = 1 \cdot 3 \cdot 5 \dots (2n-1)$. The leading oscillatory terms cancel each other.

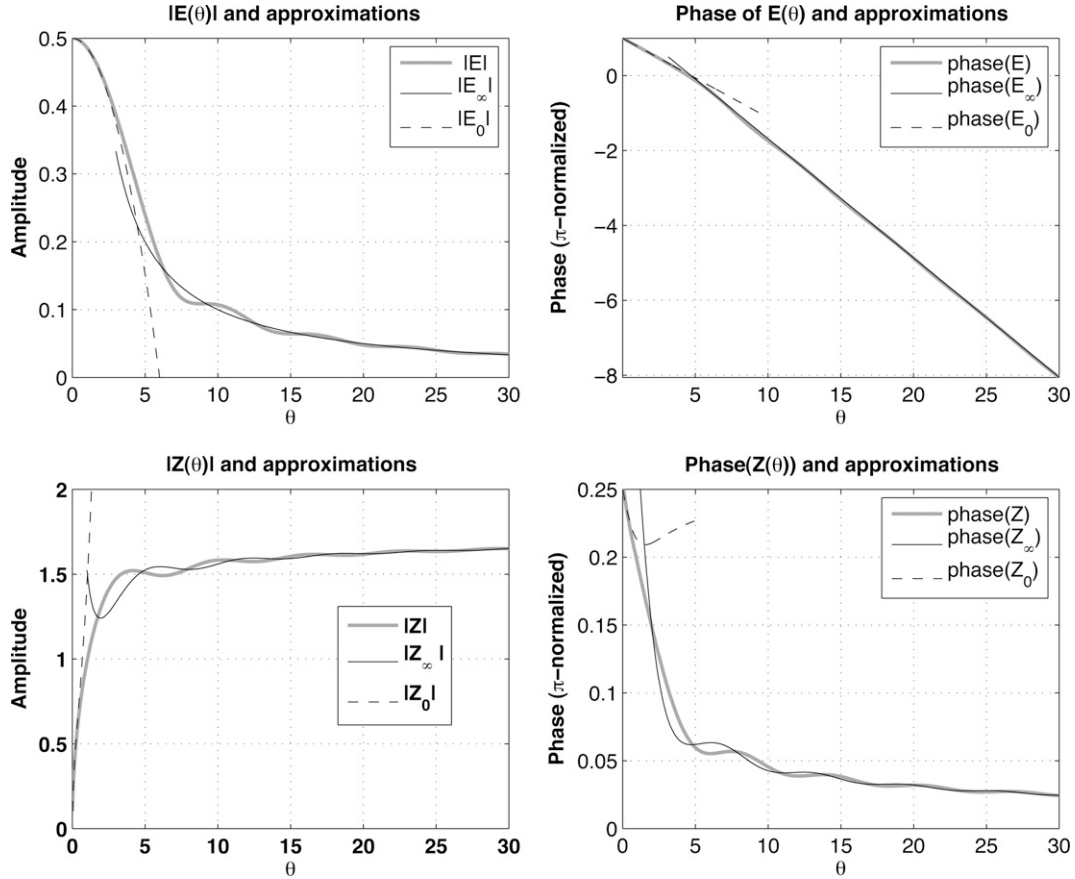


FIG. 3. Amplitude and phase of the functions E and Z , which characterize the response via h_E . Along the functions are their asymptotic expansions for large and small θ , denoted by the subscripts ∞ and 0 , respectively. (See text for details.)

Eq. (7) and the work of CS81, who considered such an unbounded basin.

The function Z is plotted in Fig. 3, along with its asymptotic approximations. We see that the asymptotic approximations are quite good. Note that Z is nonzero unless $\theta = 0$. It has a number of local minima [cf. Eq. (19)] but all are quite shallow, so the value of Z at these minima is not very different from that at neighboring points. There are no true basin modes; zeroes of Z require that θ be complex, with $\Im(\theta) > 0$, which means that the associated eigenmodes will be damped.

c. The forced solution: Green's function

We seek the response to a delta function in latitude: a Green's function. We take $F(y) = \delta(y - y_*)/X_E$ so that the integral of F over the basin is unity. Kuklinski (1984) solved the related problem of a delta function at a point, $F(y) = \delta(y - y_*) \delta(x - x_*)$, while Jin and Neelin (1993) solved the problem $F(x, y) = \delta(x - x_*)$. We will first solve the problem for a meridionally in-

nite basin and then argue that the same solution applies in the bounded basins of interest here.

The solution for a general $F(y)$ may be written, following CS81 [their Eq. (12), together with (14) and (21)],

$$\mathbf{u}_F = \frac{e^{i\omega t}}{i\phi} [d_K \mathbf{K}(y) (1 - e^{-i\phi\xi}) + \sum_{n=0}^{\infty} r_n \mathbf{R}_n(y) (1 - e^{i(2n+1)\phi\xi})], \quad (22)$$

where $\mathbf{K}(y)$ and $\mathbf{R}_n(y)$ are the meridional structures associated with the Kelvin mode and the n th Rossby mode, respectively. (See CS81 for details.) The coefficients d_K and $\{r_n, n \in \mathbb{N}\}$ are the projections of the forcing onto the Kelvin and Rossby modes. For the Green's function $F(y) = \delta(y - y_*)/X_E$, they are

$$d_K = K^u(y_*), \quad (23a)$$

$$r_n = \frac{4n(n+1)}{2n+1} R_n^u(y_*), \quad (23b)$$

where K^u , R_n^u denote the u components of the Kelvin wave and the n th Rossby wave. We need only the western boundary mass flux:

$$\begin{aligned} e^{i\omega t} I_F &= \int_{-\infty}^{\infty} u_F(x=0) dy, \\ &= \pi^{1/4} \frac{e^{i\omega t}}{i\phi} \left[K^u(y_*) (1 - e^{i\phi}), \right. \\ &\quad \left. - 2 \sum_{n=0}^{\infty} \alpha_n R_n^u(y_*) \frac{1 - e^{-i(2n+1)\phi}}{2n+1} \right], \end{aligned} \quad (24)$$

where α_n is the sequence defined as

$$\alpha_n = \begin{cases} 0, & n \text{ even} \\ (2\pi^{1/4})^{-1} \int_{-\infty}^{\infty} y \psi_n(y) dy, & n \text{ odd.} \end{cases} \quad (25)$$

[ψ_n is the n th Hermite function, as defined, e.g., in Abramowitz and Stegun (1965)]. Equation (24) can be rewritten as

$$\begin{aligned} I_F &= \pi^{1/4} \frac{i}{\phi} \int_0^{\phi} d\phi' [K^u(y_*) e^{i\phi'} \\ &\quad + 2 \sum_{n=0}^{\infty} \alpha_n R_n^u(y_*) e^{-i(2n+1)\phi'}]. \end{aligned} \quad (26)$$

Once again, the term in brackets is the sum of a free Kelvin mode and its Rossby reflections, this time evaluated at the forcing latitude y_* . Again, we use the result of Cane and Moore (1981) to rewrite it as in (5):

$$I_F = \frac{i}{\phi} \int_0^{\phi} d\phi' \tan(2\phi') [\cos(2\phi')]^{1/2} e^{-iy_*^2 \tan 2\phi'/2}. \quad (27)$$

Remarkably, the mass flux due to the forced mode simply writes as the integral of the free-mode zonal flux over $[0, \phi]$. This integral has no obvious analytical simplification, but in the limit of small ϕ becomes

$$I_F = \frac{2i}{\phi} \int_0^{\phi} \phi' e^{-i\phi' y_*^2} d\phi'. \quad (28)$$

An integration by part leads to

$$I_F = \frac{-2}{y_*^2} \left[e^{-iy_*^2 \phi} + \frac{i}{y_*^2 \phi} \left(1 - e^{-iy_*^2 \phi} \right) \right]. \quad (29)$$

We now define the function E :

$$E(\theta) = \left[\frac{1 - e^{-i\theta}}{\theta^2} + \frac{e^{-i\theta}}{i\theta} \right] \quad (30)$$

so that I_F can be written

$$I_F = -2i\phi E(\phi y_*^2). \quad (31)$$

Before we examine E more closely, we wish to justify applying this solution in a bounded basin. We argue heuristically that the solutions do not spread poleward enough to be aware of the boundaries; that is, they do not generate any motions at the boundary that require boundary layer corrections. If the forcing latitude is far from the equator ($y_* \gg 1$), then the motions are going to be geostrophic, the linear planetary geostrophic equations hold, and the wave operator $y^2 h_t - h_x$ allows only propagation along latitude lines so that the signal cannot spread poleward. On the other hand, if the forcing is in low latitudes, then it has a very small projection onto the high n modes, that is, the ones that do not die off exponentially at middle latitudes. The result that the forced motions will not be significant far poleward of the forcing can also be argued from results on ray paths of equatorial waves (Kuklinski 1984; Schopf et al. 1981). Only in the case of a forcing reaching the boundary of the basin does the solution require a boundary layer correction; it is presented in appendix A. Finally, our results agree with the closed basin solutions of L03 and CL01, as we will show in the next section.

We plot the function E in Fig. 3 and note some of its properties:

- for $\theta \ll 1$, $E_0 \sim -1/2 + i(\theta/3) + (\theta^2/8)$, so $|E_0| \sim 1/2 (1 - (\theta^2/36))$, $\varphi(E_0) \sim \pi - 2\theta/3$, wherein φ is the phase;
- for $\theta \gg 1$, $|E_\infty| \sim 1/\theta$, $s\varphi(E_\infty) \sim 3\pi/2 - \theta$;
- $|E|$ decreases strongly with θ . Thus, for a given frequency, low-latitude winds are more efficient at generating thermocline motion than high-latitude winds.

d. Total solution

In the case of a symmetric basin ($y_S = -y_N$) and a delta-function forcing, we can use expressions (13) and (31) for the free and forced mass fluxes to rewrite (4) into the following form, which is the Green's function of the eastern boundary height:

$$h_E^*(\phi, y_*) = \sqrt{i\phi} \frac{E(\phi y_*^2)}{Z(\phi y_N^2)}, \quad (32)$$

which depends solely on the frequency, basin size, and latitude of the forcing, y_* . Thus, for an arbitrary wind

profile $F(y)$, the total solution is simply F weighted by the integral kernel h_E^* :

$$h_E(\phi) = \int_{y_s}^{y_N} F(y_*) h_E^*(\phi, y_*) dy_*,$$

$$= \frac{2\sqrt{i\phi}}{Z(\phi y_N^2)} \int_0^{y_N} F(y_*) E(\phi y_*^2) dy_*. \quad (33)$$

This expression is new, and it allows a systematic evaluation of the equatorial thermocline response to arbitrary wind forcings. It is to be compared with the response functions given by Eq. (2.8) in L03 or Eq. (23) in CL01 (the latter two being identical except for notation). The denominator is identical in all expressions for $\phi \ll 1$, so the difference resides in the numerator: as is traditional in quasigeostrophic (QG) theory, L03 and CL01 express the wind forcing as an Ekman pumping term $[-\partial_y (F/y)$ in our notation], while we use no such transformation. Their choice makes direct computations challenging if F is nonzero at the equator, while ours circumvents this limitation. Were our results to be recast in a similar form, we would obtain an expression nearly identical to theirs, differing only by an extra term multiplying the Ekman pumping within the integrand. Consequently, we obtain very similar results in cases where $F \sim y$ at the equator, but not otherwise (section 4). This is therefore a more general solution.

3. Results

a. Low versus midlatitudes

The first result of interest, and the one that motivated this paper, is the sharp decrease of E with latitude for a given frequency, as seen in Fig. 3 (recall that $\theta \sim y^2$). Here, $|E(\theta)|$ falls to half its value from $\theta = 0$ at approximately $\theta = 5$. For a 20-yr period in the Pacific this corresponds to a latitude of $\sim 43^\circ$. This means that the equatorial thermocline is best excited locally in the tropics; subtropical or midlatitude wind forcing is less effective. As has been known for a long time, the longer the period, the broader the range of latitudes that influence the equator. In agreement with earlier work, we find that the latitudinal extent increases like the square root of the period. While it is true then that the lower the frequency, the greater the impact of midlatitude winds; tropical winds always have the advantage.

An alternative explanation of the relative ineffectiveness of midlatitude winds can be derived from midlatitude quasigeostrophic theory: Consider a 1.5-layer β -plane ocean. Suppose there is a midlatitude pycnocline displacement h , which is zero outside of some latitude band (y_-, y_+) . The equatorial response (i.e., the Kelvin

wave amplitude) is set by the magnitude of the total mass flux U impinging on the western boundary. Using geostrophy,

$$U \approx \int_{y_-}^{y_+} \frac{g}{f} h_y dy = - \left[\frac{g}{f} h \right]_{y_-}^{y_+}$$

$$- \int_{y_-}^{y_+} g\beta \frac{h}{f^2} dy = - \int_{y_-}^{y_+} g\beta \frac{h}{f^2} dy, \quad (34)$$

which is small—the *quasi* in quasigeostrophic. Therefore, the higher the latitude of the forcing, the less the impact at the western boundary and, therefore, at the equator. For a fixed width $(y_+ - y_-)$, we again have the result that the impact decreases like the square of the latitude. This result comes out of an inviscid theory and would be even more relevant in the presence of damping; since the Rossby wave crossing time increases quadratically with latitude, midlatitude forcing is also more severely damped by the time it reaches the eastern boundary.

b. Modes do not matter

We have seen that the free mode amplitude depends on the mass flux at the western boundary that the wind forcing excites. The larger this mass flux, the larger the free mode amplitude. If an off-equatorial forcing excites a direct response that by itself satisfies the free mode condition that the net mass flux at the western boundary be zero, then it will have no impact on the equator. Of course, there are no true free modes since all eigensolutions with frequency greater than zero are damped. This is true even in the infinite basin case in which the free mode is an artifact of the low-frequency, long-wave approximation (cf. CM81). Moreover, as shown in CM81, even the “true” modes of the approximate equations all have periods shorter than interannual.

In a closed basin, there are pseudomodes with complex frequencies, as emphasized by CL01 and L03. Such modes would be important if they meant that I_M was especially close to zero for corresponding real frequencies. However, they introduce only small amplitude oscillations in $Z(\phi y_N^2)$, hence in h_E (cf. Fig. 3). We also point out that a combination of basin size and frequency that minimizes I_M and, so, increases H_E does so equally for forcings at all latitudes. It does not favor midlatitudes.

c. Response to idealized wind patterns

It is instructive to look at simple wind patterns, the response to which may be obtained analytically via

(33), for simple enough functional forms. A useful identity is

$$\forall \theta > 0, \forall \nu \in \mathbb{C}^*, \int_0^\theta \frac{e^{-\nu \vartheta}}{\sqrt{\vartheta}} d\vartheta = \frac{1}{\sqrt{\nu\pi}} \operatorname{erf}(\sqrt{\nu\theta}), \quad (35)$$

through which the various integrals can be computed. In all the following, a white spectrum for the forcing is implicitly assumed, as in CL01 and L03. This should not be thought of as a naïve simplification of reality, as it is known that the spectrum of midlatitude surface winds is far from flat, with significant power in the ENSO band. Instead, the idea is to see whether this low frequency variability can arise *via* the amplification of stochastic wind forcing by ocean dynamics alone. Since synoptic weather systems are known to occur spontaneously with approximately Gaussian statistics, this is meant to provide a null hypothesis for the redness of the CTI spectrum.

1) RESPONSE TO $F = 1$

Let us consider the simplest forcing:

$$F = \begin{cases} 1, & \text{for } y \in [-L, L] \\ 0, & \text{otherwise.} \end{cases} \quad (36)$$

The analytical response to such forcing is

$$h_E = \frac{2\sqrt{i\theta_L}E(\theta_L) + \sqrt{\pi} \operatorname{erf}(\sqrt{i\theta_L})}{Z(\theta_N)}, \quad (37)$$

where $\theta_N = \phi y_N^2$ and $\theta_L = \phi L^2$. This case provides a useful cross check because the zero frequency is easy to compute without recourse to our theory: if such a steady forcing were to cover the whole basin, then the slope of the equatorial thermocline depth would be unity by virtue of the Sverdrup balance; there would be a node in the center of the basin, and $h_E = 1/2$. Using the previous expansions for E and Z in the limit of small θ , and the results from the appendix, one can verify that the response to a steady forcing ($\phi = 0$) is, indeed, $h_E = 1/2$ for this solution.

In Figs. 4a1),a2), we show the spectrum of the response to a varying latitudinal extent of this forcing, with

$$\frac{L}{y_N} = \frac{1}{3}, \frac{2}{3}, s1,$$

respectively. For $L = y_N$, the forcing is nonzero at the northern wall so that the boundary layer correction needs to be applied, as outlined in the appendix. It is interesting to note that a spectral peak does arise for periods in the range between 10- and 20-yr, but only in the case of tropical forcing. The more poleward the

forcing, the weaker the peak and the lower its central frequency so that basinwide forcing alone does not, in fact, produce a peak anymore. The subtropical case produces a peak in the 50–100-yr range. As the extent of the forcing increases, it eventually comes close enough to the northern boundary so that the boundary layer correction has to be applied. It is a peculiarity of this Heaviside forcing, with a sharp jump introducing an infinite wind stress curl at the edge, that the interior and boundary layer contributions are of similar magnitude when $L = y_N$ and tend to cancel each other (see the appendix). This explains the decrease between the zero-frequency response to $L = 2y_N/3$ (black solid line) and $L = y_N$ (black dashed line) in Fig. 4a2.

However, the comparison between latitude bands is not very meaningful in this case where the area under the forcing keeps increasing with its extent. Instead, one can divide the domain in three equal chunks, called for convenience “tropics,” “subtropics,” and “midlatitudes.” (Recall that the convergence of meridians is neglected in the β -plane approximation.) This is done in Figs. 4b1) and b2), where it can be seen that the shift of the peak toward low frequencies is indeed a consequence of the location of the forcing, not its extent (the more poleward it is, the lower the frequency). In this case, the midlatitude spectrum shows a peak around 50–100-yr periods, like the subtropical case, only weaker in magnitude.

One can verify that this result is not an artifact of the chosen functional form, by applying another one—say, a sine wave—similarly cut into latitude bands [Figs. 4c1) and c2)]: the amplitude of the thermocline response increases in proportion to the strength of the forcing over a given region, but the location of the peaks is the same as in the $F = 1$ case. In fact, in this case, the midlatitude forcing fails to produce a peak.

As remarked above, a caveat of such forcings is that they possess a discontinuous first derivative, which introduces an infinite wind stress curl, and is therefore unphysical. For the purposes of comparison with earlier work and numerical testing, it is instructive to look at a smooth forcing.

2) RESPONSE TO $F(y) = e^{-\mu(y^2/2)}$

In this case, as in the $L = y_N$ case seen above, the forcing is nonzero at the northern wall, requiring the boundary layer correction. However, for μ large enough, this correction is evanescent. The solution is

$$h_E = \frac{i^{1/2}}{Z(\theta_N)} \left[\frac{\sqrt{\pi}}{2} p^{1/2} + K(\mu, \phi, y_N) \exp\left(-\mu \frac{y_N^2}{2}\right) \right], \quad (38)$$

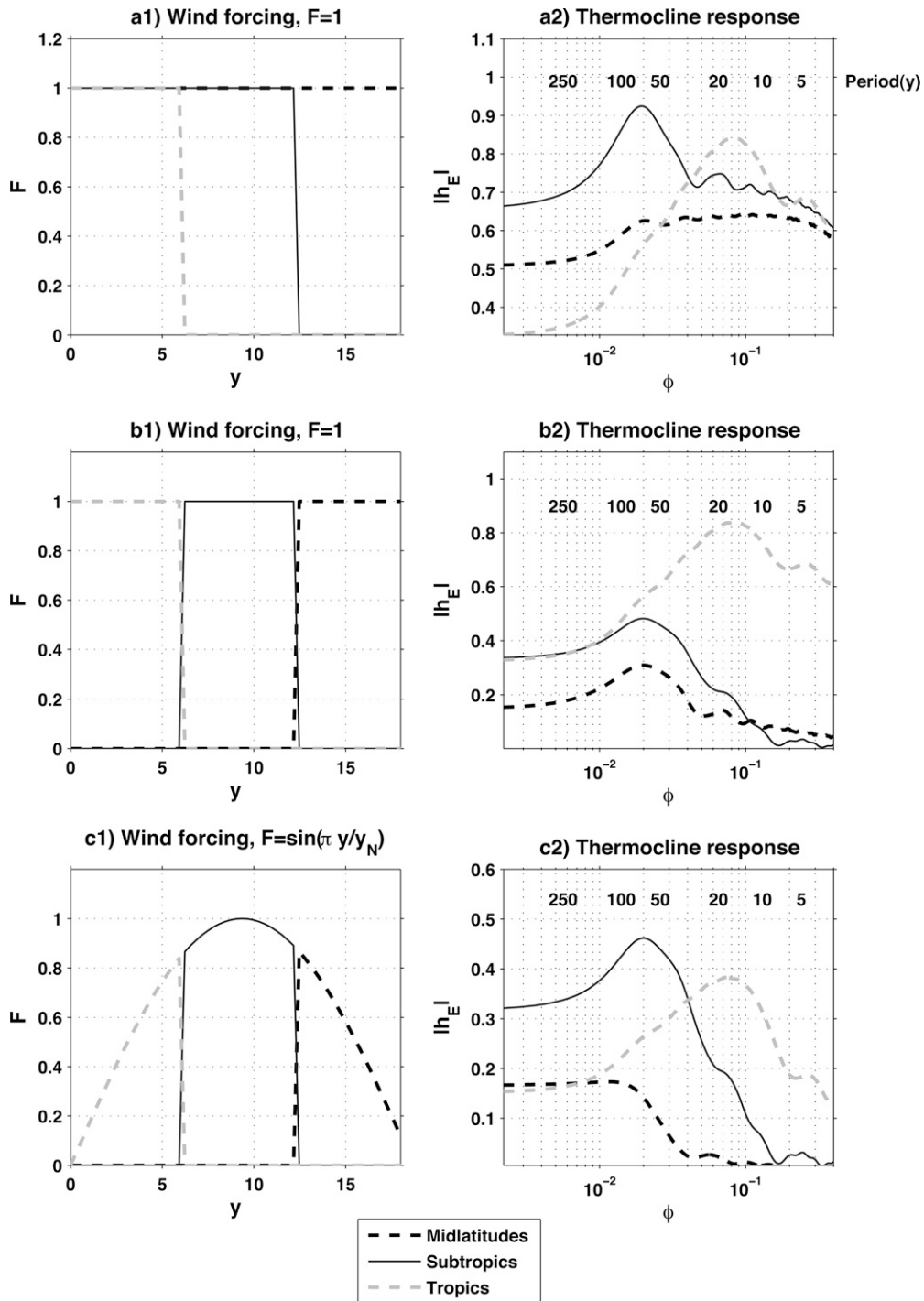


FIG. 4. Effect of the latitudinal position of the wind forcing: a1) Varying extent of wind forcing in the $F = 1$ case; a2) thermocline response; b1) varying location of wind forcing in the $F = 1$ case; b2) thermocline response; c1) varying location of wind forcing in the $F = \sin(\pi y/y_N)$ case; c2) thermocline response. The numbers above the spectra on the rhs correspond to the period of oscillation (yr).

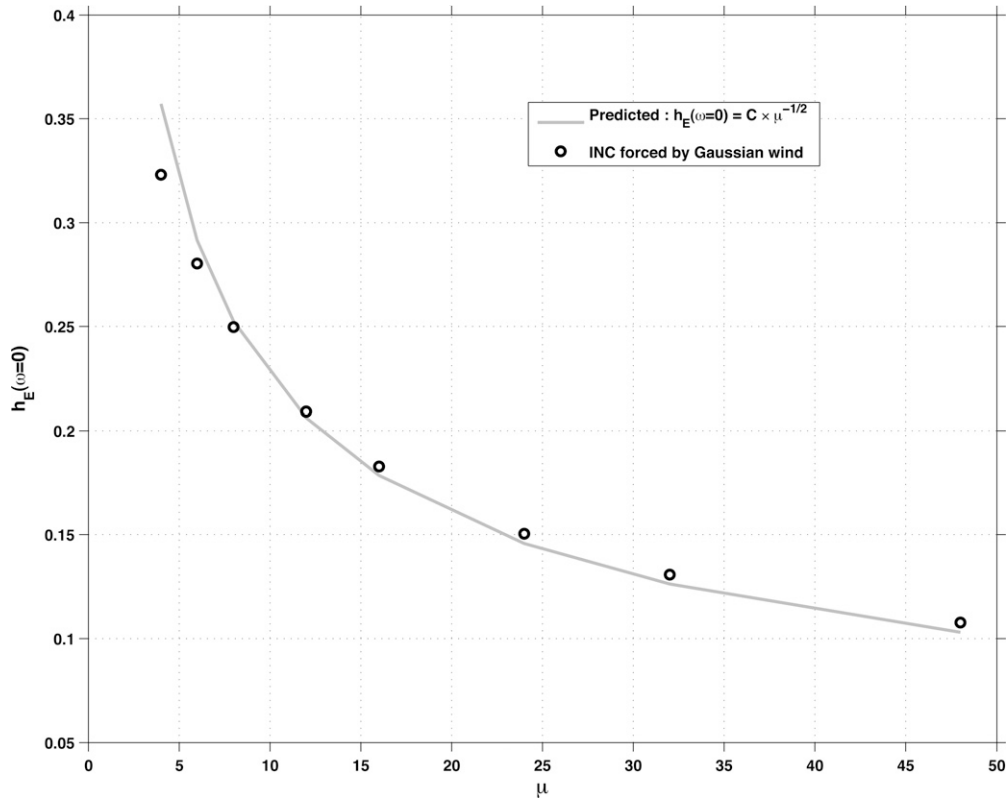


FIG. 5. Response of the INC model to $F = e^{-\mu y^2}/2$ for varying values of the width parameter μ . The values of h_E plotted here are the average over the last year of a 200-yr integration of the shallow-water solver INC (Israeli et al. 2000) with a constant forcing applied. The model was run in a symmetric basin with $y_N = 60^\circ\text{N}$ and Rayleigh friction $r = 50 \text{ yr}^{-1}$.

where $p = 2\phi/\mu$ as in CS81, and

$$\begin{aligned} \mathbf{K}(\mu, \phi, y_N) = & \frac{2p^{-1/2}}{3} \left(\frac{1 - e^{-i\theta_N}}{i\theta_N} \right) - \frac{\sqrt{\theta_N}}{3} E(\theta_N) \\ & - \frac{i}{2\sqrt{\theta_N}} \left(1 - \frac{1 - e^{-i\theta_N}}{i\theta_N} \right). \end{aligned} \quad (39)$$

Since $\mathbf{K} e^{-\mu y_N^2/2} \rightarrow 0$ as $y_N \rightarrow \infty$, the solution reduces to

$$h_E = \frac{p^{1/2}}{2} e^{i\pi/4}, \quad (40)$$

which is identical to Eq. (31) in CS81. For a bounded basin ($y_N < \infty$) and $\phi \ll 1$, the lowest order response simplifies to

$$\lim_{\phi \rightarrow 0} h_E = \left(\frac{2\pi}{\mu y_N^2} \right)^{1/2}. \quad (41)$$

Note that according to Eq. (41), h_E is equal to the integral of $F(y)$ divided by y_N and is thus independent of the scale of the forcing with the total amplitude held

fixed. Remarkably, it is independent of ϕ . We find, therefore, an $O(1)$ zero frequency response, which contrasts with CS81 but is a consequence of their considering an unbounded basin, where mass within any finite region need not be conserved. We checked this behavior in a numerical model using the INC scheme (Israeli et al. 2000). In Fig. 5 we plot the equilibrium response of this model. The $\mu^{-1/2}$ scaling law form is found to hold over a broad parametric range.

4. Comparison with previous work

Since our results are in stark contrast with the claims of CL01 and L03, we dedicate this section to understanding the origin of the difference.

a. Comparison with Liu

It is instructive to see to what extent our solution resembles that of L03. In Fig. 6 we reproduce the results from his Fig. 5, using the methods of this paper. For this computation we used his ideal wind forcings

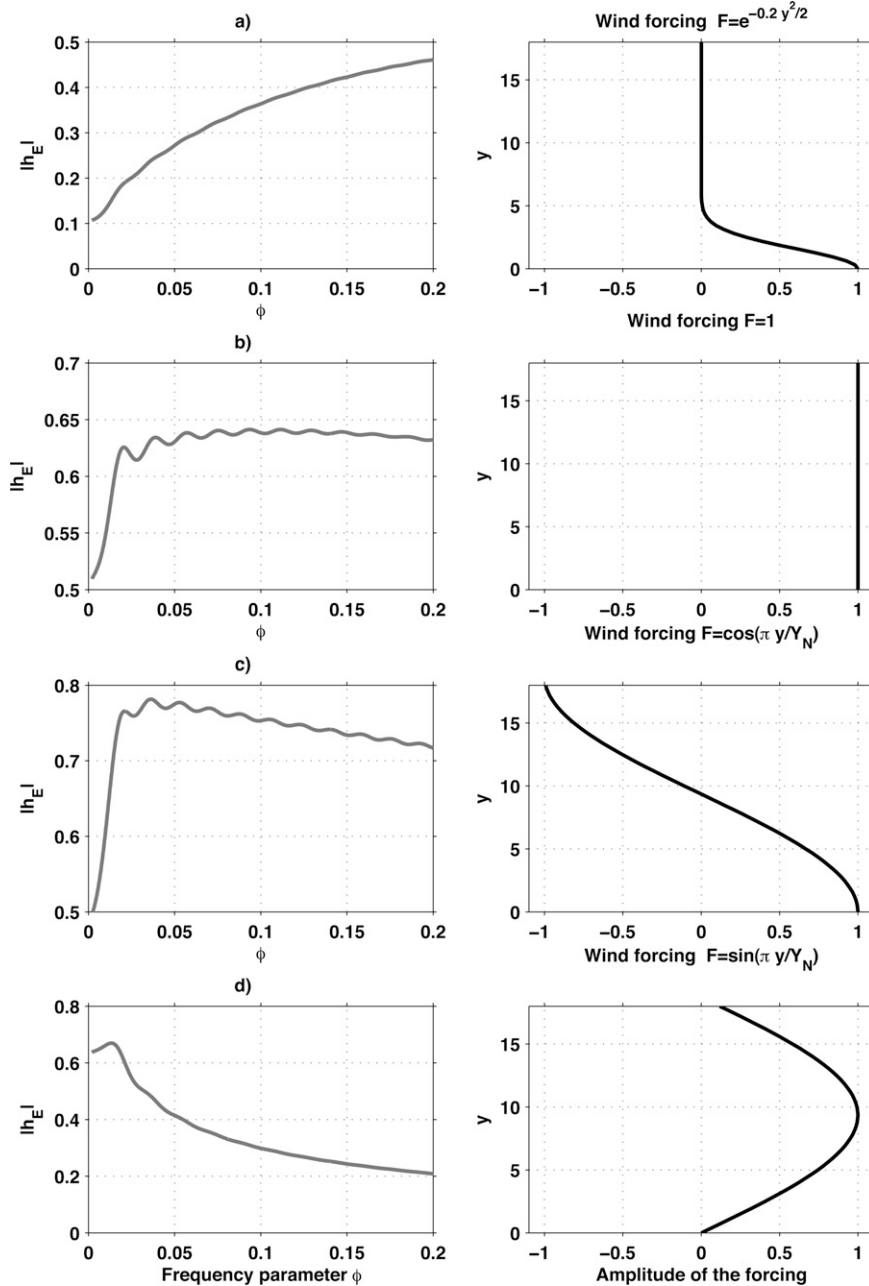


FIG. 6. Reproduction of Fig. 5 in L03. The rhs presents the forcing (a) $F(y) = e^{-\mu y^2/2}$, (b) $F(y) = 1$, (c) $F(y) = \cos[\pi(y/y_N)]$, and (d) $F(y) = \sin[\pi(y/y_N)]$, respectively. The lhs presents the corresponding thermocline response.

and the Green's function obtained from (27), complemented by the boundary layer correction (see the appendix) when needed.

Except for a few minor differences in amplitude, the two pictures are in good agreement, especially for case d $F(y) = \sin(\pi y/y_N)$. When they are not, case c, $[F(y) = \cos(\pi y/y_N)]$, it is likely to be related to the fact that L03's HE and HP solutions diverge from each other,

presumably due to a singularity in the forcing used at the equator (one that corresponds to an infinite Ekman pumping, as illustrated by the dashed lines in the right-hand side of his Fig. 5a-c). When the latter Ekman pumping is nonsingular, his HP and our solution are in close agreement. For well-behaved cases, we agree with L03's conclusion that equatorial wave theory and planetary geostrophy give identical results at very low fre-

quencies. As we shall see in the section 5, it is our interpretation that differs.

b. Comparison with Cessi and Louazel

This comparison is complicated by the fact that the wind patterns prescribed as a forcing of the planetary geostrophic potential vorticity (PGPV) equation, their Eq. (19), are specified in terms of the function $\tilde{g} \equiv (F/y)_y$ (in our notation). As this involves a differential, an integration constant is needed to fully determine F . Furthermore, one can show that all of the wind patterns used in their study imply that F scales at least as y^2 as one approaches the equator. Any lesser-order polynomial would render the solution singular. These wind patterns have far greater amplitude in high latitudes, so this part of the wind forcing naturally dominates.

However, if a more realistic wind pattern were chosen, one characterized by a comparable amplitude in midlatitudes and the equator, then the PGPV solution would not show enhanced sensitivity to extratropical winds, because it behaves similarly to the equatorial wave solution at low frequencies, as explained by Liu (2003). The reason for this similarity deserves a formal explanation.

c. Equivalence with the PGPV solution

SCALING ARGUMENTS

Why does the PGPV equation seem to capture the thermocline motion of the equatorial wave solution at very low frequencies? A formal way to see this is to show that it is a special case of the low-frequency, long-wave approximation. Recall that the latter is obtained by using the following scaling (Cane and Sarachik 1976):

$$\begin{aligned} \frac{\partial}{\partial t} &\sim O(\varepsilon), & \frac{\partial}{\partial x} &\sim O(\varepsilon), & \frac{\partial}{\partial y} &\sim O(1), \\ u, h &\sim O(1), & v &\sim O(\varepsilon), \end{aligned} \quad (42)$$

wherein ε is a small parameter. This scaling makes v_t appear as $O(\varepsilon^2)$, and must therefore be dropped to lowest order.

At very low frequencies [$\partial_t \sim O(\varepsilon^2)$], consistency requires adding the constraint $\partial_y \sim O(\varepsilon)$ and so, for $y \geq O(1)$, (1c) implies that $u \sim \varepsilon h$. Hence u_t must also be dropped to lowest order, yielding the planetary geostrophic equations:

$$-yv = -h_x + F(y, t), \quad (43a)$$

$$yu = -h_y, \quad (43b)$$

$$h_t + u_x + v_y = 0. \quad (43c)$$

The immense advantage of this system is that a vorticity equation can be formed for h , which is readily integrable. It is surprising that this equation should be valid near the equator ($y \ll 1$), however, since the Rossby wave speed there goes to infinity. L03 showed that the planetary geostrophic solution accounts implicitly for the mass transport achieved by the equatorial Kelvin wave and retains the essential Sverdrup balance in the vicinity of the equator. The reason for the consistency between very-low-frequency linear equatorial wave theory and planetary geostrophy is that, in both theories, the equatorial thermocline depth must proceed from the balance $h_x = F$. Direct integration from the eastern boundary yields

$$h = h_E + (x - X_E)F, \quad (44)$$

where it can be seen that h_E is simply the constant of integration of the problem, which is determined by the boundary conditions. As we show in section 2b, the two theories have the same boundary conditions for low frequencies, hence their similar behavior.

5. Discussion

We have investigated the sensitivity of the equatorial thermocline depth to wind forcing at various latitudes. Following previous work, we used a β -plane nondissipative shallow-water system and showed that its solution can be approximated by a closed-form expression in the limit of low frequencies. Throughout this derivation we have made extensive use of the results of CS81 and CM81, but our solution now applies to a bounded basin, not an infinite one—via a boundary layer correction. This implicitly introduces friction in the model, albeit concentrated at the domain edges. The resulting modes are thus no longer limited to those identified by CM81, whose lowest frequency is on the order of 8 months. Indeed, the solution reproduces the salient aspects of those obtained by CL01 and L03, but also holds at shorter periods (seasonal to interannual), though in this work we only make use of the very low-frequency approximation.

Since the fundamental variable describing the response is $\theta = \phi y^2$, this means that the latitudinal range affected by the waves is proportional to the square root of their period: the longer the period, the broader the meridional extent of the wave, and the easier it becomes to force h_E from higher latitudes. However, contrary to the suggestion of CL01 and L03, we find pseudomodes unable to redden the response to a mid-latitude wind forcing with a white spectrum, nor do they introduce noticeable spectral peaks.

Further, we computed the Green's function of the

problem, which exhibited a rapid decrease with latitude. This suggested that the equatorial thermocline response inherently favors local forcing and that tropical winds dominate the response on interannual to decadal time scales. Midlatitude winds are hard pressed to produce any sizable equatorial response, unless one looks at very low frequencies, low enough for θ to be small at those latitudes. In dimensional units, this corresponds to periods from 50 to 100 yr. In such a case, Rossby waves have the time to cross the basin at the poleward boundaries within a period of oscillation, and we do find that subtropical and midlatitude winds are thus able to generate power in the centennial band. So, in our model at least, it seems that tropical winds are the preferred way of generating tropical ocean decadal variability, but modes could play a role at lower frequencies.

Might this conclusion carry over to the Pacific Ocean as a whole? While seemingly simplistic, reduced-gravity models have proven to be a surprisingly valuable interpretive tool in tropical oceanography, their applicability to midlatitude oceans is less clear. We argue that shallow-water basin modes are unlikely to be operating in nature, for three reasons.

First, as one appeals to the spatial structure of eigenmodes to generate a response, the exact geometry of the basin becomes crucial to their reinforcement: the straight coastlines used in this model are known to be a singular case of quasigeostrophic dynamics (Primeau 2002) characteristic of midlatitude oceans. For realistic Pacific coastlines, his study found that basin modes are still present in the reduced-gravity context, but with a Q factor of order one: in other words, they are far from resonance and hence offer no outstanding advantage in forcing tropical motion. Second, since the Rossby wave crossing time increases quadratically with latitude, the presence of any small amount of friction (or other diabatic processes) will tend to damp such modes much more efficiently than it would damp a dynamically forced response confined to the equatorial waveguide. Lastly, LaCasce and Pedlosky (2004) have shown in a two-layer quasigeostrophic context that Rossby waves are vulnerable to destruction by baroclinic instability. As the growth rate of this instability increases approximately quadratically with latitude (Eady 1949), there exists a critical latitude beyond which Rossby waves “succumb to baroclinic instability” and transfer most of their energy to the barotropic eddy field (LaCasce and Pedlosky 2004) before propagating too far from the eastern boundary, letting the authors conclude that “Rossby basin modes, if they exist, would be limited to tropical domains.”

Therefore, this simple model suggests that the most direct origin for decadal thermocline variability is decadal wind variability occurring in the tropics themselves (see also Karspeck and Cane 2002). Where, in turn, does such variability arise? We argue that midlatitude oceans need not be invoked to explain its origin. It has been shown that the Bjerknes feedback central to ENSO physics also operates on decadal and interdecadal time scales in the Zebiak–Cane model (Zebiak and Cane 1987; Clement and Cane 1999; Seager et al. 2004) as well as in a coupled GCM (Vimont et al. 2003). Thus coupled ocean–atmosphere dynamics internal to the tropical Pacific can produce significant power at decadal frequencies, with simulated variability resembling that observed (Karspeck et al. 2004), including the 1976–77 “climate shift.” In turn, ocean–atmosphere feedbacks involving the eastern subtropical Pacific may explain some attributes of the PDV (Wang et al. 2003a,b). It is also plausible that some elements of subtropical stochastic variability participate in this, as in the “seasonal footprinting mechanism” (Vimont et al. 2001) and the “Pacific meridional mode” (Chiang and Vimont 2004). Work reported here advances these ideas only indirectly, by ruling out resonant ocean basin modes as a viable null hypothesis for the origin of Pacific decadal variability.

Acknowledgments. J.E.G. would like to thank Ed Sarachik for an illuminating discussion; Colin Stark and Jason Smerdon, Gustavo Correa, Naomi Naik, Jennie Velez, and Lawrence Rosen for invaluable technical assistance. J.E.G. was supported by the Boris Bakhmeteff Fellowship in Fluid Mechanics and NOAA Grant 198364826.

APPENDIX

Boundary Layer Correction

When the forcing reaches the poleward boundaries of the domain, the forced solution (31) has to be amended. Our solution holds within a distance ε of the northern wall so that we can write the interior western boundary mass flux for half the basin as

$$U_I = 2i\phi \int_0^{ym-\varepsilon} F(y)E(\phi y^2) dy. \quad (A1)$$

Far from the equator the PGPV solution holds to lowest order:

$$h = \pi \left(\frac{F}{y}\right)_y \left(\frac{1 - e^{i\phi y^2 \xi}}{i\phi}\right), \quad (A2)$$

and the boundary layer zonal mass flux can be computed using geostrophy:

$$u = -\frac{1}{y}h_y, \quad (\text{A3})$$

so

$$U_\varepsilon = \left[-\frac{h}{y} \right]_{y_N-\varepsilon}^{y_N} + \int_{y_N-\varepsilon}^{y_N} \frac{h}{y^2} dy. \quad (\text{A4})$$

Taking $F = 0$ at $y = y_N - \varepsilon$ since it is already included in the interior integral, performing another integration by parts, and using the previous formula (A1) for U_I , the boundary layer return flow is

$$U_\varepsilon = -\frac{h_N}{y_N} + \frac{F_N}{y_N} \left(\frac{1 - e^{-i\theta_N}}{i\theta_N} \right) - 2i\phi \int_{y_N-\varepsilon}^{y_N} F(y)E(\phi y^2) dy, \quad (\text{A5})$$

where $F_N = F(y_N)$. We can ignore the integral, which is approximately $-2i\phi \varepsilon F_N E(\theta_N) \approx O(\varepsilon)$. Again, using (A2) to compute the meridional mass flux at the northern wall,

$$V_N = \int_{-1}^0 v d\xi = \frac{1}{y_N} \left(\int_{-1}^0 h_\xi d\xi - \int_{-1}^0 F d\xi \right), \\ = \frac{h_N - F_N}{y_N}. \quad (\text{A6})$$

Therefore, the total boundary layer correction is

$$U_\varepsilon + V_N = -\frac{F_N}{y_N} \left(1 - \frac{1 - e^{-i\theta_N}}{i\theta_N} \right) \quad (\text{A7})$$

so that, for a symmetric basin ($y_S = -y_N$), the total mass flux is

$$I_F = -2 \left\{ i\phi \int_0^{y_N} F(y)E(\phi y^2) dy + \frac{F_N}{y_N} \left[1 - \frac{1 - e^{-i\theta_N}}{i\theta_N} \right] \right\}, \quad (\text{A8})$$

which reduces to (31) if the forcing vanishes at the boundary ($F_N = 0$).

For $\theta_N \geq 1$, one can obtain a crude estimate of the importance of the boundary forcing as follows:

$$F_B \sim 2 \frac{F_N}{y_N}, \quad F_I = 2i\phi y_N F$$

[using $E = O(1)$] so that

$$\frac{F_B}{F_I} \sim \frac{1}{\theta_N} \leq 1, \quad (\text{A9})$$

which confirms the intuitive result that for basins sufficiently large, the effect of the northern and southern boundary mass fluxes is less than that of the interior mass flux.

This intuition fails, however, when $\phi \rightarrow 0$ so that θ_N becomes small. In this case the interior term [first term on the rhs of (A8)] is just $-i\phi y_N \bar{F}$, where \bar{F} is the meridional average of $F(y)$, and the boundary term is $i\phi y_N F_N/2$, so the two terms are comparable, and $h_E \rightarrow \bar{F} - F_N/2$.

REFERENCES

- Abramowitz, M., and I. A. Stegun, 1965: *Handbook of Mathematical Functions*. National Bureau of Standards Applied Mathematics Series, Vol. 55, Dover Publications, 11 046 pp.
- Cane, M. A., and E. S. Sarachik, 1976: Forced baroclinic ocean motions. 1. Linear equatorial unbounded case. *J. Mar. Res.*, **34**, 629–665.
- , and —, 1977: Forced baroclinic ocean motions. 2. Linear equatorial bounded case. *J. Mar. Res.*, **35**, 395–432.
- , and D. W. Moore, 1981: A note on low-frequency equatorial basin modes. *J. Phys. Oceanogr.*, **11**, 1578–1584.
- , and E. S. Sarachik, 1981: The response of a linear baroclinic equatorial ocean to periodic forcing. *J. Mar. Res.*, **39**, 651–693.
- Cessi, P., and S. Louazel, 2001: Decadal oceanic response to stochastic wind forcing. *J. Phys. Oceanogr.*, **31**, 3020–3029.
- , and F. Paparella, 2001: Excitation of basin modes by ocean-atmosphere coupling. *Geophys. Res. Lett.*, **28**, 2437–2441.
- , and F. Primeau, 2001: Dissipative selection of low-frequency modes in a reduced-gravity basin. *J. Phys. Oceanogr.*, **31**, 127–137.
- Chiang, J. C. H., and D. J. Vimont, 2004: Analogous Pacific and Atlantic meridional modes of tropical atmosphere ocean variability. *J. Climate*, **17**, 4143–4158.
- Clement, A., and M. A. Cane, 1999: A role for the tropical Pacific coupled ocean-atmosphere system on Milankovitch and millennial timescales. Part I: A modeling study of tropical Pacific variability. *Mechanisms of Millennial-Scale Global Climate Change*, *Geophys. Monogr.*, Vol. 29, Amer. Geophys. Union, 363–372 pp.
- Deser, C., and J. M. Wallace, 1990: Large-scale atmospheric circulation features of warm and cold episodes in the tropical Pacific. *J. Climate*, **3**, 1254–1281.
- Eady, E. T., 1949: Long waves and cyclone waves. *Tellus*, **1**, 33–52.
- Ghil, M., and Coauthors, 2002: Advanced spectral methods for climatic time series. *Rev. Geophys.*, **40**, 1003, doi:10.1029/2000RG000092.
- Israeli, M., N. H. Naik, and M. A. Cane, 2000: An unconditionally stable scheme for the shallow water equations. *Mon. Wea. Rev.*, **128**, 810–823.
- Jiang, N., J. D. Neelin, and M. Ghil, 1995: Quasi-quadrennial and quasi-biennial variability in the equatorial Pacific. *Climate Dyn.*, **12**, 101–112.
- Jin, F.-F., 2001: Low-frequency modes of tropical ocean dynamics. *J. Climate*, **14**, 3874–3881.
- , and J. D. Neelin, 1993: Modes of interannual tropical ocean-atmosphere interaction—A unified view. Part I: Numerical results. *J. Atmos. Sci.*, **50**, 3477–3503.
- Kaplan, A., M. A. Cane, Y. Kushnir, A. C. Clement, M. B. Blumenthal, and B. Rajagopalan, 1998: Analyses of global sea

- surface temperature 1856–1991. *J. Geophys. Res.*, **103**, 18 567–18 589.
- Karspeck, A. R., and M. A. Cane, 2002: Tropical Pacific 1976–77 climate shift in a linear, wind-driven model. *J. Phys. Oceanogr.*, **32**, 2350–2360.
- , R. Seager, and M. A. Cane, 2004: Predictability of tropical Pacific decadal variability in an intermediate model. *J. Climate*, **18**, 2842–2850.
- Kuklinski, R., 1984: The effect of wind measurement errors on linear simulations of equatorial circulations. M.S. thesis, Department of Meteorology, Massachusetts Institute of Technology, 156 pp.
- LaCasce, J. H., and J. Pedlosky, 2004: The instability of Rossby basin modes and the oceanic eddy field. *J. Phys. Oceanogr.*, **34**, 2027–2041.
- Liu, Z., 2003: Tropical ocean decadal variability and resonance of planetary wave basin modes. *J. Climate*, **16**, 1539–1550.
- Mann, M., and J. Lees, 1996: Robust estimation of background noise and signal detection in climatic time series. *Climatic Change*, **33**, 409–445.
- Mantua, N., and S. Hare, 2002: The Pacific Decadal Oscillation. *J. Oceanogr.*, **58**, 35–44.
- , —, Y. Zhang, J. Wallace, and R. Francis, 1997: A Pacific interdecadal climate Southern Oscillation with impacts on salmon production. *Bull. Amer. Meteor. Soc.*, **78**, 1069–1079.
- Moore, D.W., 1968: Planetary-gravity waves in an equatorial ocean. Ph.D. thesis, Harvard University, 207 pp.
- Newman, M., G. P. Compo, and M. A. Alexander, 2003: ENSO-forced variability of the Pacific Decadal Oscillation. *J. Climate*, **16**, 3853–3857.
- Primeau, F., 2002: Long Rossby wave basin-crossing time and the resonance of low-frequency basin modes. *J. Phys. Oceanogr.*, **32**, 2652–2665.
- Sarachik, E., and D. Vimont, 2003: Decadal variability in the Pacific. *Chaos in Geophysical Flows*, G. B. Boffetta et al., Eds., OTTO, 12–167.
- Schopf, P., D. L. T. Anderson, and R. Smith, 1981: Beta-dispersion of low-frequency Rossby waves. *Dyn. Atmos. Oceans*, **5**, 187–214.
- Seager, R., A. R. Karspeck, M. A. Cane, Y. Kushnir, A. Giannini, A. Kaplan, B. Kerman, and J. Velez, 2004: Predicting Pacific decadal variability. *Earth Climate: The Ocean–Atmosphere Interaction*, *Geophys. Monogr.*, Vol. 147, Amer. Geophys. Union, 105–120.
- Thomson, D. J., 1982: Spectrum estimation and harmonic analysis. *Proc. IEEE*, **70**, 1055–1096.
- Trenberth, K., and J. Hurrell, 1994: Decadal atmosphere-ocean variations in the Pacific. *Climate Dyn.*, **9**, 303–319.
- Vimont, D. J., D. S. Battisti, and A. C. Hirst, 2001: Footprinting: A seasonal connection between the tropics and mid-latitudes. *Geophys. Res. Lett.*, **28**, 3923–3926.
- , —, and —, 2003: The seasonal footprinting mechanism in the CSIRO general circulation models. *J. Climate*, **16**, 2653–2667.
- Wang, X., F.-F. Jin, and Y. Wang, 2003a: A tropical ocean recharge mechanism for climate variability. Part I: Equatorial heat content changes induced by the off-equatorial wind. *J. Climate*, **16**, 3585–3598.
- , —, and —, 2003b: A tropical ocean recharge mechanism for climate variability. Part II: A unified theory for decadal and ENSO modes. *J. Climate*, **16**, 3599–3616.
- Yang, H., and Z. Liu, 2003: Basin modes in a tropical-extratropical basin. *J. Phys. Oceanogr.*, **33**, 2751–2763.
- Zebiak, S. E., and M. A. Cane, 1987: A model El Niño–Southern Oscillation. *Mon. Wea. Rev.*, **115**, 2262–2278.
- Zelle, H., G. Appeldoorn, G. Burgers, and G. van Oldenborgh, 2004: The relationship between sea surface temperature and thermocline depth in the eastern equatorial Pacific. *J. Phys. Oceanogr.*, **34**, 643–655.
- Zhang, Y., J. Wallace, and D. Battisti, 1997: ENSO-like interdecadal variability: 1900–93. *J. Climate*, **10**, 1004–1020.